Field Interpolation Across Discontinuities in FDTD

Gaetano Marrocco, *Student Member, IEEE*, Fernando Bardati, and Marco Sabbadini

***Abstract*— Primary field quantities and their derivatives, like power flux density or surface equivalent currents, are usually required in practical applications of finite-difference time domain (FDTD). The data obtained from the FDTD algorithm are therefore interpolated to provide the whole set of the electrical and magnetic field components at each grid node to evaluate them. In the presence of a material discontinuity, however, the linear interpolation, having the accuracy of the FDTD algorithm at points where the field is continuous, will fail for the components which are orthogonal to the interface. A dielectric interpolator is presented for these cases which retains accuracy by preserving the correct field discontinuities.**

***Index Terms*— Dielectric discontinuities, FDTD, field interpolation.**

I. Introduction

THE finite-difference time-domain (FDTD) method is considered a versatile and efficient tool for the solution of Maxwell's equations in complex structures for any time dependence. Applications include planar antennas, scatterers buried in the ground, indoor propagation, and power deposition inside realistic models of human body. Antenna systems can be successfully analyzed even when they radiate onto dielectrically inhomogeneous structures such as substrates, inhomogeneously filled cavities and feed-lines. Due to the leap-frog scheme, the electric and magnetic field components are evaluated by FDTD at different points of two shifted grids obtained by repetition of the elementary Yee cell [1] along the coordinate axes in such a way that no field component is computed by the algorithm at the vertices of any cell (grid points). However, many applications require the evaluation of functionals of the electric and magnetic fields, such as power loss, Poynting vector, and surface equivalent sources for near-to-far field transformation. To this aim the FDTD outcomes are interpolated in order to provide co-located electric and magnetic components [2], [3].

In this letter two common interpolation schemes will be reviewed with reference to the accuracy. Then we propose a new algorithm which is suited for interpolation across dielectric discontinuities.

II. Linear and Dielectric Interpolations

The error ε_x when an electric component, e.g., E_x, is approximated by $\hat{E}_x$ is defined as $\varepsilon_x = |E_x(\underline{r}_0, t_n) - \hat{E}_x(\underline{r}_0, t_n)|$ where $\underline{r}_0 = (x_i, y_j, z_k)$ is a grid point. t_n is a time counter and will be hereafter omitted. The piecewise (PW) approximation assumes the FDTD components to be constant along each cell side [4]. Accordingly $\hat{E}_x(\underline{r}_0) = E_x(x_i + \Delta/2, y_j, z_k)$, where the right-hand side is directly computed by FDTD, Δ is grid size. The error is

$$\varepsilon_x = |E_x(x_i, y_j, z_k) - E_x(x_i + \Delta/2, y_j, z_k)|. \tag{1}$$

An explicit dependence of ε_x on Δ can be obtained by Taylor's expansion of E_x in the neighborhood of $(x_i + \Delta/2, y_j, z_k)$:

$$E_x(x_i + \Delta/2, y_j, z_k) = E_x(x_i, y_j, z_k) + \frac{\Delta}{2} \cdot \left.\frac{\partial E_x}{\partial x}\right|_{(x_i, y_j, z_k)} + \mathcal{O}\left(\frac{\Delta}{2}\right)^2. \tag{2}$$

If E_x is continuous between $(x_i - \Delta/2, y_j, z_k)$ and $(x_i + \Delta/2, y_j, z_k)$, the derivative in (2) can be approximated according to the first-order central difference scheme

$$\left.\frac{\partial E_x}{\partial x}\right|_{(x_i, y_j, z_k)} \cong \frac{E_x(x_i + \Delta/2, y_j, z_k) - E_x(x_i - \Delta/2, y_j, z_k)}{\Delta}. \tag{3}$$

The following estimate of the error for PW approximation

$$\varepsilon_x > E_{\text{ox}} \pi \frac{\Delta}{\lambda} \tag{4}$$

can be obtained by assuming the plane monochromatic travelling-wave trial solution as was proposed by Taflove in the treatment of the numerical dispersion [5]. The error depends linearly on the cell electrical size and, as expected, vanishes as Δ/λ vanishes. Since in applications this ratio normally ranges between 1/20 and 1/10, the error is about 15%–30% of field amplitude.

A more accurate method is the linear interpolation of the data from FDTD computation. Accordingly

$$\hat{E}_x(x_i, y_j, z_k) = \tfrac{1}{2} E_x(x_i + \Delta/2, y_j, z_k) + \tfrac{1}{2} E_x(x_i - \Delta/2, y_j, z_k). \tag{5}$$

The error for linear approximation is

$$\varepsilon_x = \tfrac{1}{2} |[E_x(x_i, y_j, z_k) - E_x(x_i - \Delta/2, y_j, z_k)] - [E_x(x_i + \Delta/2, y_j, z_k) - E_x(x_i, y_j, z_k)]|. \tag{6}$$

If an expansion of E_x is performed up to the second-order terms at points $x = x_i \pm (\Delta/2)$, as in the FDTD formulation, it follows that the right-hand side of (6) vanishes within the accuracy of FDTD. Therefore, a linear interpolation exhibits

Manuscript received June 18, 1997.

G. Marrocco and F. Bardati are with DISP, University of Rome "Tor Vergata," Rome, Italy.

M. Sabbadini is with ESA-ESTEC, Noordwijk, The Netherlands.

Publisher Item Identifier S 1051-8207(98)01196-9.

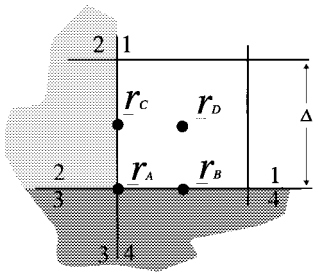

Fig. 1. Nodal points for field-component interpolation on a Yee's cell.

the same order of accuracy, in homogeneous region, as the FDTD algorithm.

The linear interpolator of a function g, at the interior points of the rectangle R, of area S, can be cast as

$$g_0 = \frac{1}{S}\sum_{p=1}^{4} S_{p0} g_p \tag{7}$$

where g_0 is the interpolation at $\underline{r}_0 \epsilon R$. Denoting two opposite vertices of R by V_p and $\overline{V}_p, g_p$ is the value of g at V_p, and S_{p0} is the area of the sub-rectangle of R, which is singled out by two coordinate lines through $\underline{r}_0$ and has $\overline{V}_p$ as a vertex. Equation (7) is general in the sense that it can be useful even in the case of a graded mesh (unequal arms of the elementary cell).

The standard linear interpolation is useful if g is continuous. This might not be the case where a region is inhomogeneous since the electric field component, which is perpendicular to the boundary between different dielectric media, is discontinuous and the normal derivative is undefined. Staircase approximation of dielectric boundaries is assumed by standard FDTD. Therefore a boundary can be classified at a given point with reference to the field component which is interpolated at that point. A two-dimensional (2-D) Yee cell is shown in Fig. 1 with four different dielectrics around $\underline{r}_A$ [a vertex of a Yee's cell can be surrounded by eight different dielectrics in a general three-dimensional (3-D) case]. The interface between media 1 and 4 is tangential for E_x at $\underline{r}_B$, while the interface between 1 and 2 is normal for E_x at $\underline{r}_C$. The discontinuity at $\underline{r}_A$ will be referred to as a mixed discontinuity. Notice that $E_x(\underline{r}_B)$ is directly computed by FDTD, while $E_x(\underline{r}_A), E_x(\underline{r}_C)$ and $E_x(\underline{r}_D)$ must be interpolated if they are of interest. Since the cell is homogeneously filled, (7) can be used for $E_x(\underline{r}_D)$.

An interpolator for points on normal and mixed boundaries can be obtained by enforcing the continuity of the normal component of $\underline{D} = \hat{\epsilon}\underline{E}$ where $\hat{\epsilon} = \epsilon_0\epsilon_{\text{eff}} - j\sigma_{\text{eff}}/(2\pi f)$ is the complex effective permittivity which takes the dielectric discontinuities into account and f is frequency. The effective permittivity, ϵ_{eff}, can be obtained [6], [7] as

$$\epsilon_{\text{eff}} = \frac{(\epsilon_1+\epsilon_2)(\epsilon_3+\epsilon_4)}{\epsilon_1+\epsilon_2+\epsilon_3+\epsilon_4} \tag{8}$$

in the case of four different dielectrics. A similar formula holds for σ_{eff}. The new interpolator, for any orientation of the field component with regard to a dielectric interface, can be cast as

$$E_\ell(\underline{r}_0) = \frac{1}{S}\sum_{p=1}^{4} S_{p0}\left(\frac{\hat{\epsilon}(\underline{r}_p)}{\hat{\epsilon}(\underline{r}_0)}\right)^{\alpha} E_\ell(\underline{r}_p) \tag{9}$$

where $\ell = x, y, z, \alpha = 1$ for normal and mixed discontinuities and $\alpha = 0$ elsewhere. Equation (9) generalizes (7) to include normal and mixed boundaries across $\underline{r}_0$.

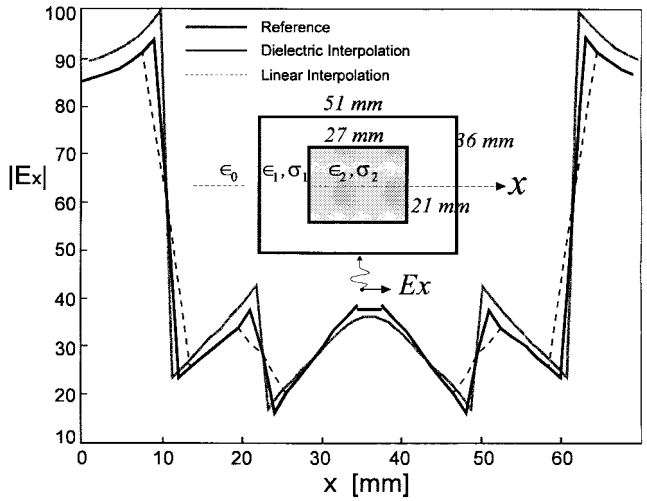

Fig. 2. $|E_x|$ versus x for a layered cylinder illuminated by a x-polarized y-directed plane wave at 3 GHz. $\epsilon_1 = 15, \epsilon_2 = 4, \sigma_1 = 0.1$ S/m, $\sigma_2 = 0.3$ S/m.

III. Numerical Examples

The accuracy of both the linear interpolator (LI) and the new dielectric interpolator (DI) has been tested by comparison with the results obtained via the standard FDTD on a finer grid. A first case was a stratified rectangular infinite cylinder illuminated by a x-polarized plane wave propagating along the positive y direction. Plots of $|E_x|$ as function of the position along the x axis are shown in Fig. 2. The reference solution was obtained from standard FDTD with $\lambda/\Delta = 20$. A second computation was performed via FDTD with doubled grid size. The results of the coarser grid simulation were interpolated according to the LI and the DI schemes. Improvement due to DI with respect to LI is apparent from the diagrams. In particular the discontinuities of E_x are better approximated by the dielectric interpolator while they are smoothed by LI. We introduce a weighted measure of the difference of two sets of results, $E_{\ell,ij}$ and $E^{(\text{ref})}_{\ell,ij}$, from 2-D numerical computations as

$$\varepsilon_{\ell,\text{rms}} = \sqrt{\frac{\sum_{ij} W_{ij}|E_{\ell,ij} - E^{(\text{ref})}_{\ell,ij}|^2}{\sum_{ij} W_{ij}|E^{(\text{ref})}_{\ell,ij}|^2}} \tag{10}$$

where $E^{(\text{ref})}_{\ell,ij}$ is the reference, i.e., the finer-grid solution. The sum is over all the nodes and W_{ij} is a region-of-interest matrix. It is worth noticing that the linear interpolator gives worst results in the vicinity of normal or wedge discontinuities. To highlight the effects on accuracy of the dielectric interpolator, W_{ij} is one on normal or wedge discontinuities, and zero

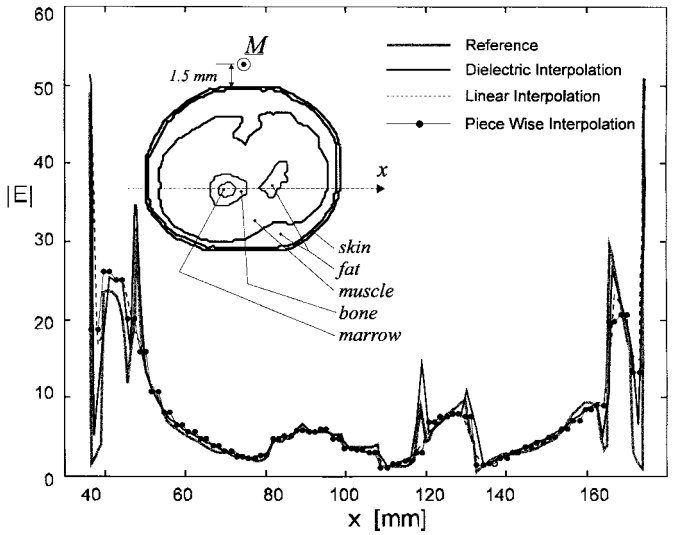

Fig. 3. $|E|$ versus x for a 2-D human thigh model irradiated by a magnetic current wire at 432 MHz. Skin: $\epsilon = 41, \sigma = 1.0$ S/m; fat: $\epsilon = 4.7, \sigma = 0.07$ S/m; muscle: $\epsilon = 44, \sigma = 1.4$ S/m; bone: $\epsilon = 8.4, \sigma = 0.15$ S/m; marrow: $\epsilon = 5.8, \sigma = 0.07$ S/m.

elsewhere. $\varepsilon_{x,\mathrm{rms}} = 0.19$ and 0.10, $\varepsilon_{y,\mathrm{rms}} = 0.21$ and 0.09 for LI and DI, respectively ($\varepsilon_{x,\mathrm{rms}} = 0.15$ and 0.12, $\varepsilon_{y,\mathrm{rms}} = 0.17$ and 0.11 for LI and DI, respectively, if $W_{ij} = 1$ over the whole domain). Therefore the results of the numerical analysis show a 100% improvement of accuracy in terms of weighted rms error.

As a second test, a functional of the field components was evaluated for a model of human thigh irradiated by an infinitely long wire with uniform magnetic current at 432 MHz (hyperthermia frequency). The problem is intrinsically 3-D but, in order to simplify the computation of the reference solution on a very dense grid, a 2-D geometry was considered resulting in a TE_z problem. An FDTD computation was performed on a $\Delta_1 = 3$-mm grid and staircase approximation of the dielectric boundary. Then E_x and E_y were interpolated according to PW, linear, and dielectric schemes, and finally, the electric field amplitude was computed for the three approximations. The reference solution was obtained for the same structure via a standard FDTD on a denser grid ($\Delta_2 = \Delta_1/4$) and electric field amplitude computed.

Plots of $|E|$ as function of the position along the x axis are shown in Fig. 3. It can be appreciated from the diagrams that the dielectric interpolator is generally superior to the other schemes in reproducing the discontinuities of $|E|$. To confirm this result, weighted errors $\varepsilon_{\mathrm{rms}}$ were evaluated for $|E|$ according to (10). We obtained: $\varepsilon_{\mathrm{rms}} = 0.22, 0.17$, and 0.10 for PW, LI, and DI, respectively, and for $W_{ij} = 1$ on the skin layer, and zero elsewhere.

IV. Conclusions

We have discussed three algorithms for the interpolation of FDTD solutions at points of the Yee's grid. The PW interpolation of a field component is affected by an error which is larger than 15% of the noninterpolated value. Moreover, the error depends on the discretization in use. The linear interpolation scheme exhibits the same order of accuracy as the FDTD algorithm and is a good choice where the field components are continuous. However, it fails in the presence of normal or mixed dielectric discontinuities. To overcome this, a new dielectric interpolator has been introduced which preserves the electric-field normal discontinuities. Numerical tests of the dielectric interpolator on 2-D problems show a $>$60% improvement in the accuracy, in terms of weighted rms error, with respect to the linear scheme.

References

[1] K. S. Yee, "Numerical solution of initial value problem involving Maxwell's equations in isotropic media," *IEEE Trans. Antennas Propagat.*, vol. AP-14, pp. 302–307, 1966.
[2] J. Fang and D. Xeu, "Numerical errors in the computation of impedences by FDTD method and ways to eliminated them," *IEEE Microwave Guided Wave Lett.*, vol. 5, pp. 6–8, Jan. 1995.
[3] W. K. Gwarek and M. Cheluch-Marcysiak, "A differential method of reflection coefficient extraction from FDTD simulations," *IEEE Microwave Guided Wave Lett.*, vol. 6, pp. 215–217, May 1996.
[4] D. Sullivan, "Three-dimensional computer simulation in deep regional hypertermia using the finite-difference time-domain," *IEEE Trans. Microwave Theory Tech.*, vol. 38, pp. 204–211, Feb. 1990.
[5] A. Taflove, *Computational Electrodynamics—The Finite-Difference Time-Domain Method*. Norwood, MA: Artech House, 1995.
[6] M. Cheluch-Marcysiak and W. K. Gwarek, "Higher-order modeling of media interfaces for enhanced FDTD analysis of microwave circuits," in *Proc. European Microwave Conf.*, 1994, Cannes, France.
[7] G. Marrocco, "FDTD modeling of dielectric discontinuities," ESA Rep. 11476-95-NL-NB.